BOUNDARY-LAYER TRANSITION ON CONES NEAR
MACH ONE IN AN AEROBALLISTIC RANGE

J. Leith Potter

ARO, Inc.

VON KÁRMÁN GAS DYNAMICS FACILITY
ARNOLD ENGINEERING DEVELOPMENT CENTER
AIR FORCE SYSTEMS COMMAND
ARNOLD AIR FORCE STATION, TENNESSEE 37389

January 1975

Final Report for Period July 1, 1973 — June 30, 1974

Prepared for

ARNOLD ENGINEERING DEVELOPMENT CENTER
ARNOLD AIR FORCE STATION, TENNESSEE 37389

This report has been reviewed by the Information Office (OI) and is releasable to the National Technical Information Service (NTIS). At NTIS, it will be available to the general public, including foreign nations.

APPROVAL STATEMENT

This technical report has been reviewed and is approved for publication.

FOR THE COMMANDER

ELTON R. THOMPSON
Research and Development
   Division
Directorate of Technology

ROBERT O. DIETZ
Director of Technology

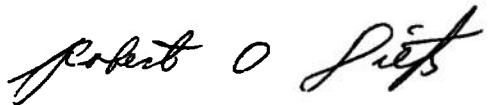| REPORT DOCUMENTATION PAGE		READ INSTRUCTIONS BEFORE COMPLETING FORM
1 REPORT NUMBER AEDC-TR-74-115	2 GOVT ACCESSION NO.	3 RECIPIENT'S CATALOG NUMBER
4. TITLE (and Subtitle) BOUNDARY-LAYER TRANSITION ON CONES NEAR MACH ONE IN AN AEROBALLISTIC RANGE		5 TYPE OF REPORT & PERIOD COVERED Final Report-July 1, 1973 to June 30, 1974
		6. PERFORMING ORG. REPORT NUMBER
7. AUTHOR(s) J. Leith Potter - ARO, Inc.		8. CONTRACT OR GRANT NUMBER(s)
9 PERFORMING ORGANIZATION NAME AND ADDRESS Arnold Engineering Development Center Arnold Air Force Station Tennessee 37389		10. PROGRAM ELEMENT, PROJECT, TASK AREA & WORK UNIT NUMBERS Program Element 65802F
11. CONTROLLING OFFICE NAME AND ADDRESS Arnold Engineering Development Center Arnold Air Force Station Tennessee 37389		12 REPORT DATE January 1975
		13. NUMBER OF PAGES 29
14 MONITORING AGENCY NAME & ADDRESS(if different from Controlling Office)		15 SECURITY CLASS. (of this report) UNCLASSIFIED
		15a. DECLASSIFICATION/DOWNGRADING SCHEDULE N/A

16. DISTRIBUTION STATEMENT (of this Report)

Approved for public release; distribution unlimited.

17. DISTRIBUTION STATEMENT (of the abstract entered in Block 20, if different from Report)

18. SUPPLEMENTARY NOTES

Available in DDC.

19. KEY WORDS (Continue on reverse side if necessary and identify by block number)

boundary layer transition
conical bodies
aeroballistic ranges

angle of attack
supersonic flow
wind tunnels

20 ABSTRACT (Continue on reverse side if necessary and identify by block number)

The feasibility of determining Reynolds numbers of boundary layer transition on sharp, 10-deg, semiangle cones at slightly supersonic free-stream Mach numbers, $1.04 \leq M_\infty \leq 1.44$, in an aeroballistic range has been demonstrated. Some problems relating to the experimental technique are discussed, and the data are compared with results for higher Mach numbers. Possibly important differences between transonic wind tunnels and the aeroballistic range

DD $_{1 \text{ JAN } 73}^{\text{FORM}}$ 1473   EDITION OF 1 NOV 65 IS OBSOLETE

20. ABSTRACT (Continued)

are pointed out in connection with a warning about comparing transition data from different facilities.

AFSC
Arnold AFS Tenn

PREFACE

The research reported herein was conducted by the Arnold Engineering Development Center (AEDC), Air Force Systems Command (AFSC), under Program Element 65802F. The results were obtained by ARO, Inc. (a subsidiary of Sverdrup & Parcel and Associates, Inc.), contract operator of AEDC, AFSC, Arnold Air Force Station, Tennessee. The work was done under ARO Project No. VF432, and the manuscript (ARO Control No. ARO-VKF-TR-74-91) was submitted for publication on September 26, 1974.

CONTENTS

ILLUSTRATIONS

Figure

1.0 INTRODUCTION

This research was done to demonstrate the feasibility of using an aeroballistic range for determining transition Reynolds numbers on axisymmetric bodies near a Mach number of one and to obtain a limited amount of data on transition in transonic flows. The results reported herein may be considered an extension of earlier studies described in Refs. 1 and 2. The experimental methods and facilities were the same, but, in the more recent work, the free-stream Mach number was reduced from $M_\infty \approx 2$ and 5 to $M_\infty \approx 1$. Consistent with the objectives of this research, only a few launches were made in the investigation. However, the results are reported because of the general interest in transonic flows and the particular value of data on transition free of the influences of transonic wind tunnel flow disturbances. This latter problem recently has been discussed by Dougherty and Steinle (Ref. 3).

2.0 EXPERIMENTAL SYSTEMS

The aeroballistic range and instrumentation related to the present report have been described in Ref. 2. No special modifications or significant procedural changes were necessary in order to conduct experiments near Mach one.

A sketch of AEDC Hyperballistic Range K is shown in Fig. 1. There are six dual-axis shadowgraph stations, two single-axis schlieren photographic stations, and one single-axis, laser-front-lighted photographic station along the length of Range K. For this experiment, the data on transition were obtained by operating the schlieren systems as focused, parallel-light shadowgraph systems.

The principal conical model is sketched in Fig. 2, and a model with its sabot is shown in Fig. 3. The cone photographed in Fig. 3 has a band of machined grooves 3.8 cm (1.5 in.) from the apex. This was done for a part of the work reported in Ref. 2 and has no connection with the present report.
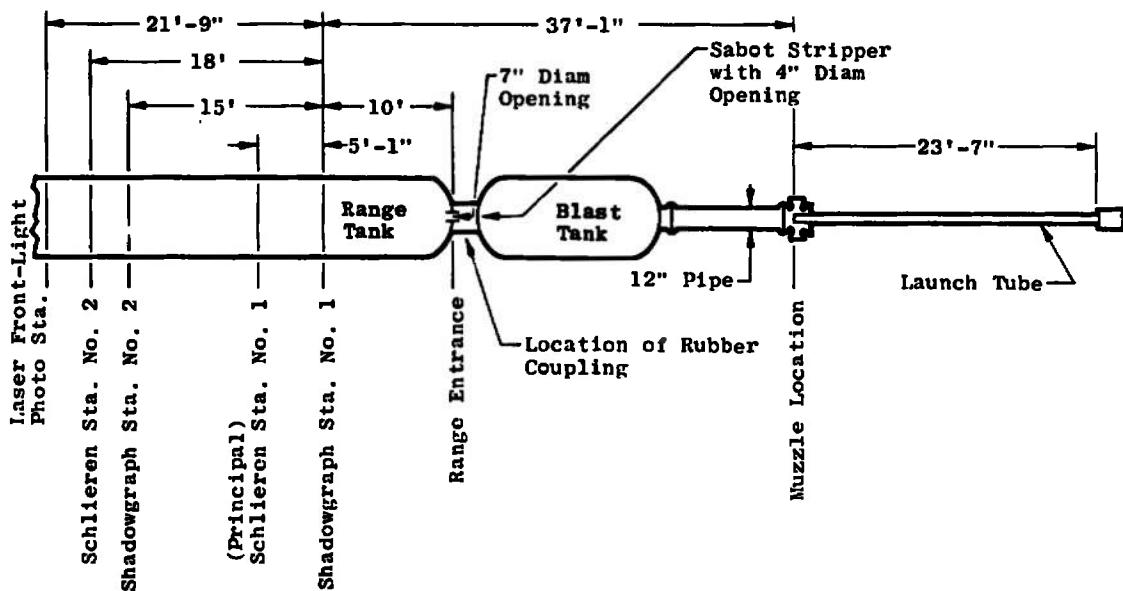
Figure 1. Schematic drawing of Range K showing uprange instrumentation and launch tube location.
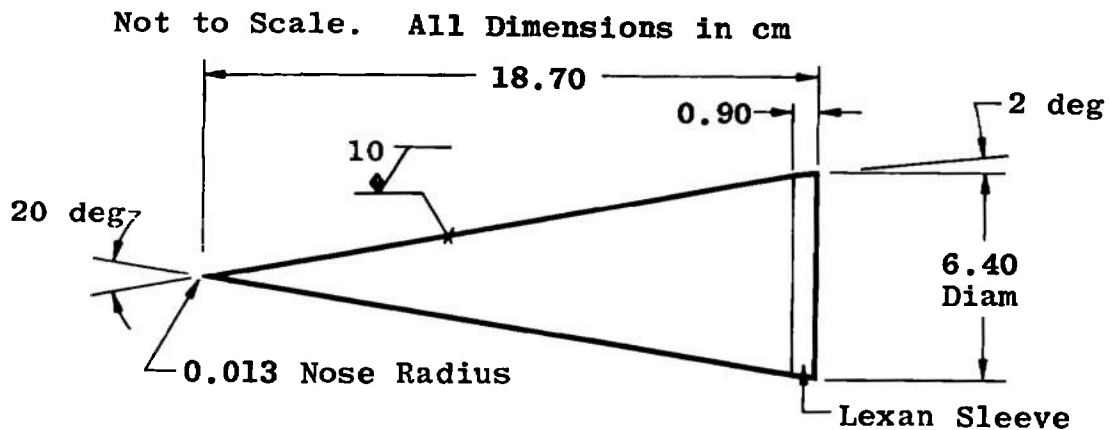

Figure 2. Aluminum cone.
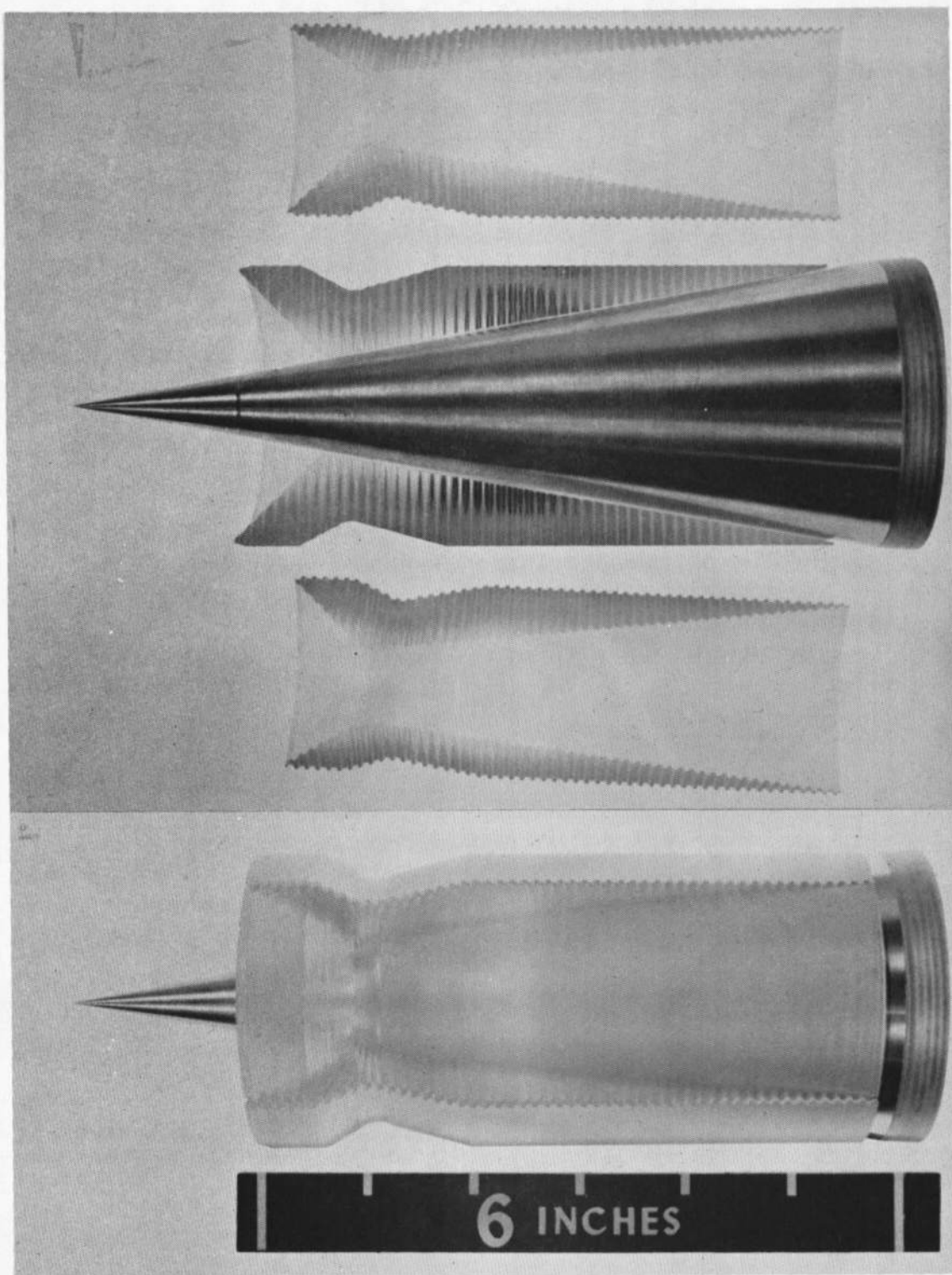
Figure 3. Cone and Sabot.

3.0 DISCUSSION OF EXPERIMENT

3.1 CONICAL FLOW CONDITION

It was desired to maintain constant or near-constant inviscid coni-
cal flow-field properties, i.e., to have attached bow shock waves.
Calculations of local Mach and Reynolds numbers are made easier
when that condition prevails, but, more importantly, the discussion of
boundary-layer transition then does not have to be complicated by in-
clusion of longitudinal pressure gradient effects. Such effects were
not altogether avoided in practice, principally because small but finite
angles of attack usually existed. However, the zero-angle flow field
was made to be conical by keeping free-stream Mach number near to
or greater than that for bow wave attachment for nominally sharp,
right circular cones of 10-deg semiapex angle.

That Mach number is not clear in the standard source (Ref. 4). In
Charts 5 and 6 of Ref. 4, one sees that the minimum value of M_∞ for
shock attachment with θ_c = 10 deg is slightly above 1.05. On the other
hand, Chart 7 shows M_∞ slightly below 1.05. With the realization that
real cone tips are not perfectly sharp and that air viscosity and non-
zero angles of attack make a fine distinction unreasonable, $M_\infty \gtrsim 1.05$
becomes an acceptable criterion for shock attachment and conical flow.

Figures 4 to 7 show examples of the cones in flight at some of the
Mach numbers investigated. At M_∞ = 1.04, Fig. 4 shows the bow shock
wave slightly curved. Because of the nose radius of curvature of
0.013 cm, the shock wave can never be attached to the apex of the cone.
In Fig. 5, the shock curvature is perhaps less, and the location of the
bow shock relative to the cone nose seems about the same as in Fig. 4.
Figure 6 represents a case at M_∞ = 1.11 where the bow shock is straight,
except very near the cone nose. However, the finite nose radius of
curvature, coupled with the greater Mach number, has caused the slightly
separated bow shock to be closely followed by a second shock on the cone
nose. These departures from ideal conical flow are of minor importance
in the context of boundary-layer transition and the calculation of corre-
sponding local flow properties several hundred nose radii downstream
of the cone apex.
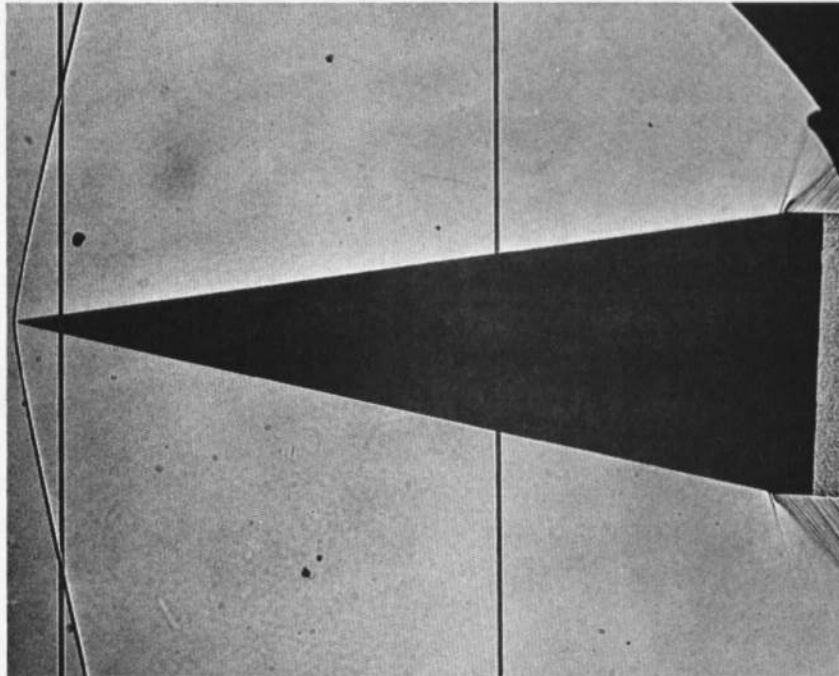
Figure 4. Cone with Mach number slightly below the shock detachment value, θ_c = 10 deg, a_p = 2.5 deg, M_∞ = 1.04.
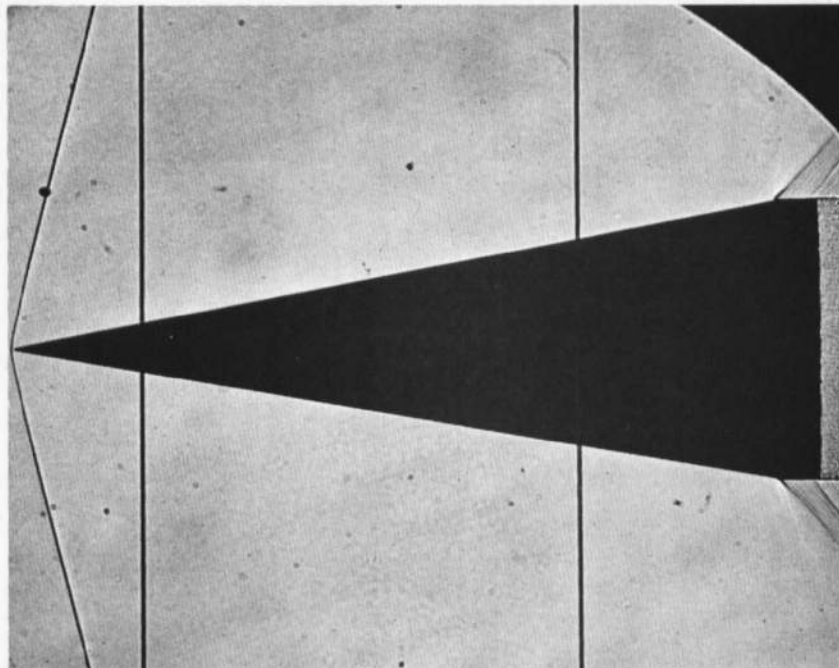
Figure 5. Cone with Mach number almost equal to the shock detachment value, θ_c = 10 deg, a_p = 0.3 deg, M_∞ = 1.05.
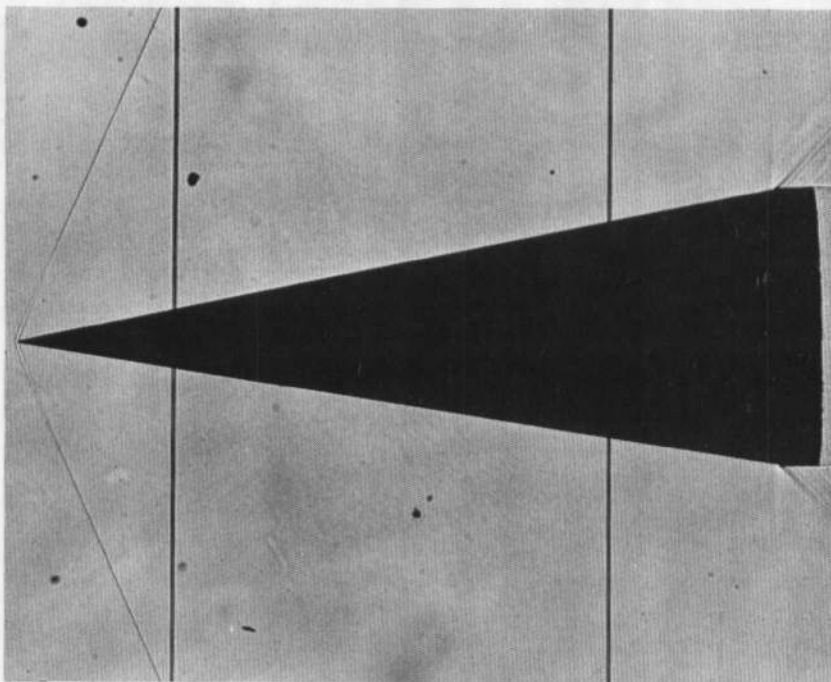
Figure 6. Cone with Mach number greater than the shock detachment value, θ_c = 10 deg, a_p = 0.7 deg, M_∞ = 1.11.
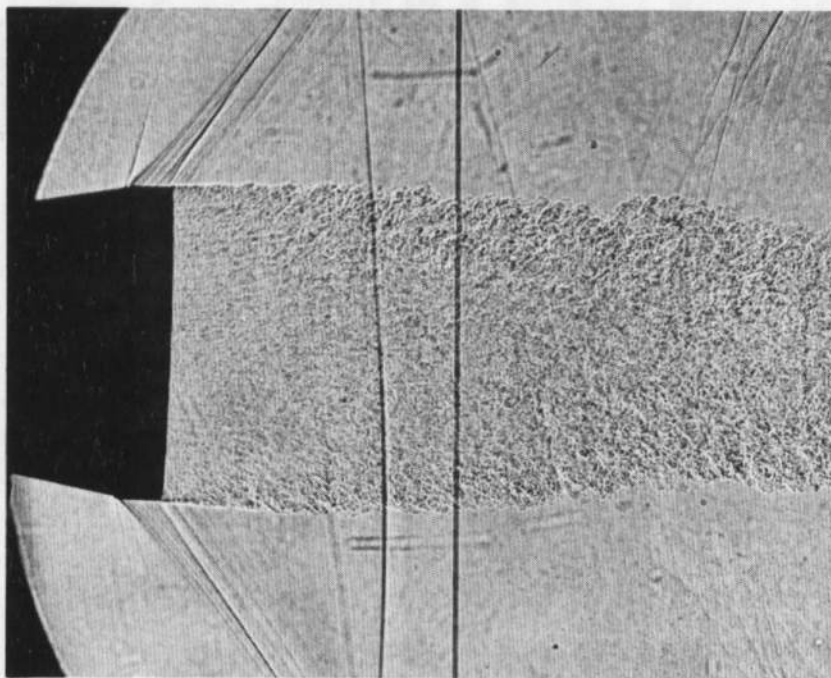
Figure 7. Cone base and wake flow at M_∞ = 1.05, θ_c = 10 deg, a_p = 0.9 deg (note bow shock reflection off window)

The freedom from interference caused by shock reflection from the range wall is explained by noting that the bow shock angle remote from the stagnation point at $M_\infty = 1.05$ is about 15 deg from a line drawn normal to the centerline. Such a shock would be reflected and return to the centerline more than one body length aft of the cone base in the present case. As an illustration of the freedom from reflected-shock interference one may use any of Figs. 4 to 6. No photographs of the reflected bow shock crossing the cone wake were obtained, but Fig. 7 shows conditions immediately downstream of the base of a cone at $M_\infty = 1.05$ where the reflection of the bow shock from the window is apparent.

Inviscid, conical-flow properties used to compute local Mach and Reynolds numbers have been obtained from a computer program prepared by AEDC (E. O. Marchand of ARO, Inc.). Figure 8 presents the results of interest in this case.
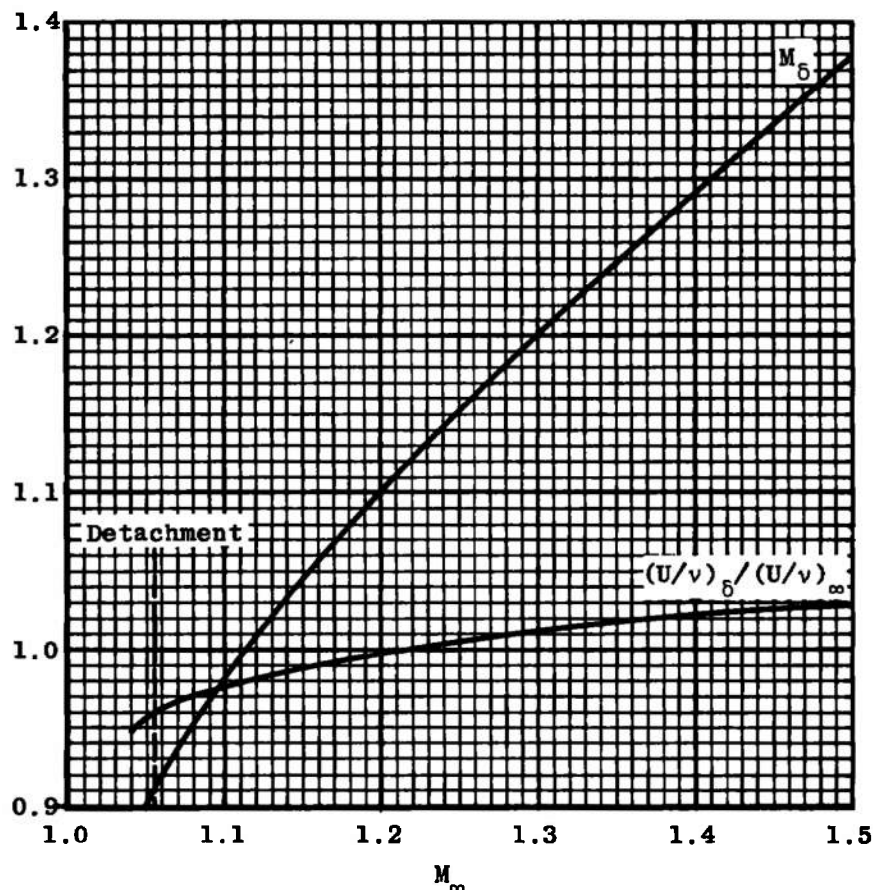
Figure 8. Mach and unit Reynolds numbers on a sharp cone of 10-deg semiapex angle at zero angle of attack in air at 297 K (535°R).

3.2 ANGLE OF ATTACK

Several factors of concern in aeroballistic investigations of transition were discussed at length in Ref. 2. Angle of attack was included in that earlier discussion, but since that time the procedure for adjusting transition Reynolds numbers to account for small angles of attack has been revised. The revised procedure will be described next. It has a broader basis in experimental data and allows treating data which would have been disallowed by the procedure followed in Ref. 2. However, comparison of the band of adjusted transition Reynolds numbers published in Ref. 2 with the same basic data after adjustment by the newer method has revealed no significant overall difference.

The principal advance over the treatment of angle-of-attack effect in Ref. 2 is in the more systematic consideration of cone meridian angles other than 0 and 180 deg. Even though the net effect on the data of Ref. 2 was negligible, the newer procedure is more generally satisfactory.

The concern over meridian angle ϕ arises because when $\alpha_p \neq \alpha$ the two longitudinal edges of the silhouette of a cone seen in a shadowgram will not correspond to ϕ = 0 and 180 deg. When $\alpha_p = \alpha$, let ϕ = 0 for the windward edge in the photograph and ϕ = 180 deg for the leeward edge. The intermediate cases are easily visualized by thinking of the limiting cases:

(1)   When $\alpha_p \equiv \alpha$, then ϕ = 0 or 180 deg

(2)   When α_p = 0 and $\alpha \neq 0$, then ϕ = ±90 deg

The lee meridian seen in a shadowgram varies between 90 and 180 deg. At the same time, the windward meridian varies from 90 to 0 deg.

In Fig. 9, data on the angle-of-attack influence on transition for ϕ = 0 and 180 deg are presented. The three experiments chosen for representation in Fig. 9 do not match the present Mach number, but more nearly comparable flow conditions with equal data are unknown to the writer. It will be noticed that the agreement of the data is relatively good for this type of experiment. On the windward side, the results obtained by Ward and Mateer are in exceptionally close agreement.

The purpose of the examination of data from wind tunnels is to establish a procedure for "adjusting" the free-flight range data to a zero-angle-of-attack status. The next step is to decide which of the curves

in Fig. 9 will be adopted. The somewhat arbitrary choice is made to use Ward's curve. It is seen to represent a reasonable compromise in regard to the other data in Fig. 9, and the unit Reynolds number, in particular, is closer to the values of that parameter for the free-flight data.

Sym	θ_c, deg	M_δ	$(U/\nu)_\delta$ in.$^{-1}$	References
O	4	2.15	4.5×10^5	Kendall (Ref. 5)
□	10	2.03	4.5×10^5	Kendall (Ref. 5)
―――	10	4.00	11×10^5	Ward (Ref. 6)
――・―	15	4.97	$1-6 \times 10^6$	Mateer (Ref. 7)
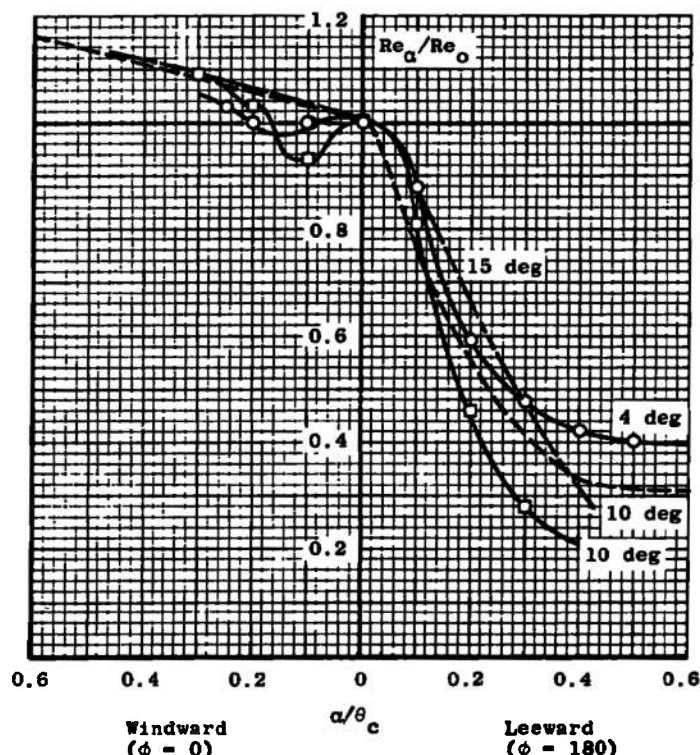
Figure 9. Selected data on the angle-of-attack influence.

Information on the variation of transition location with ϕ is contained in the papers by Mateer (Ref. 7) and DiCristina (Ref. 8). Figure 10 shows a comparison of their results and some disagreement is evident. Perhaps the wisest thing to say regarding the disagreement is that it implies decreased likelihood of repeatability or regularity of transition locations when, say, $60 < \phi < 180$. In the absence of any persuasive evidence suggesting the superiority of one of the sets of data in Fig. 10, an average has been taken. Specifically, the following s_t/s_{to} values were averaged:

(1)   Mateer's ϕ = 0 and DiCristina's ϕ = 0

(2)   Mateer's ϕ = 60 taken as given

(3)   Mateer's ϕ = 90 and DiCristina's ϕ = 108

(4)   Mateer's ϕ = 120 and DiCristina's ϕ = 144

(5)   Mateer's ϕ = 180 and DiCristina's ϕ = 180
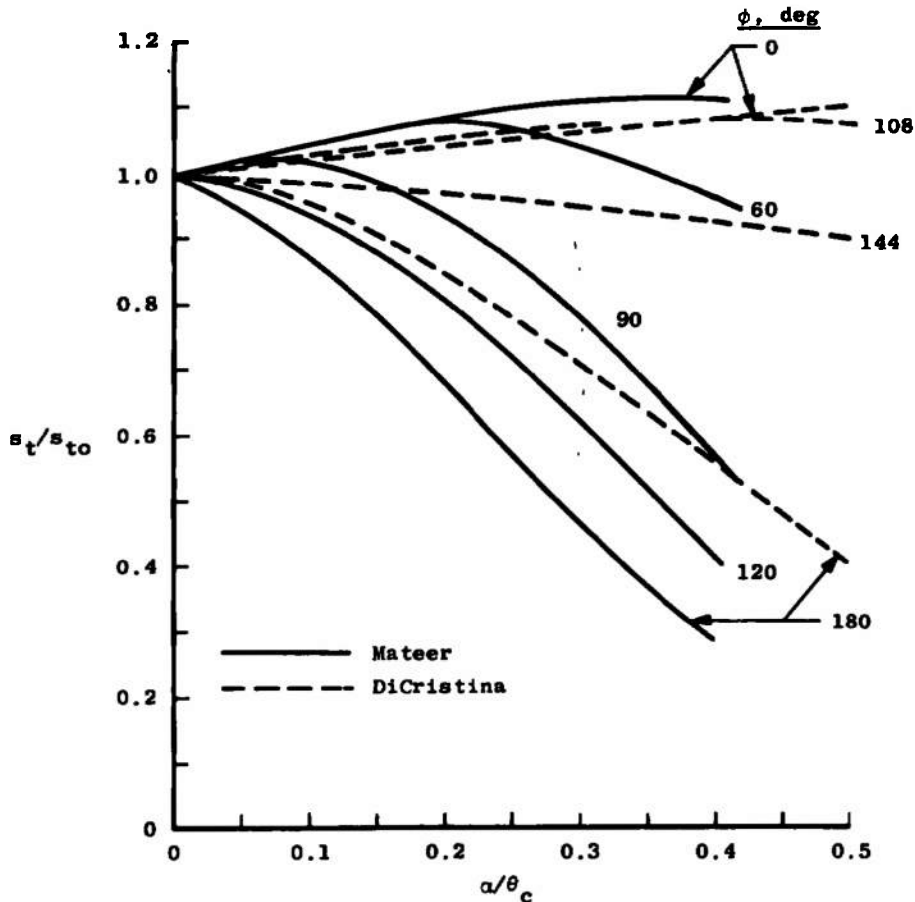
Figure 10. Comparison of results obtained by Mateer (Ref. 7)
and DiCristina (Ref. 8).

The results are displayed in Fig. 11. Not only do the curves for $60 \le \phi \le 120$ deg represent the averages of the data in Fig. 10, but they also have been adjusted by a few percent so that the ϕ = 0 and 180 deg curves in Fig. 11 agree with Ward's data. The ϕ = 150 deg curve was interpolated as a convenience in later use of the figure.
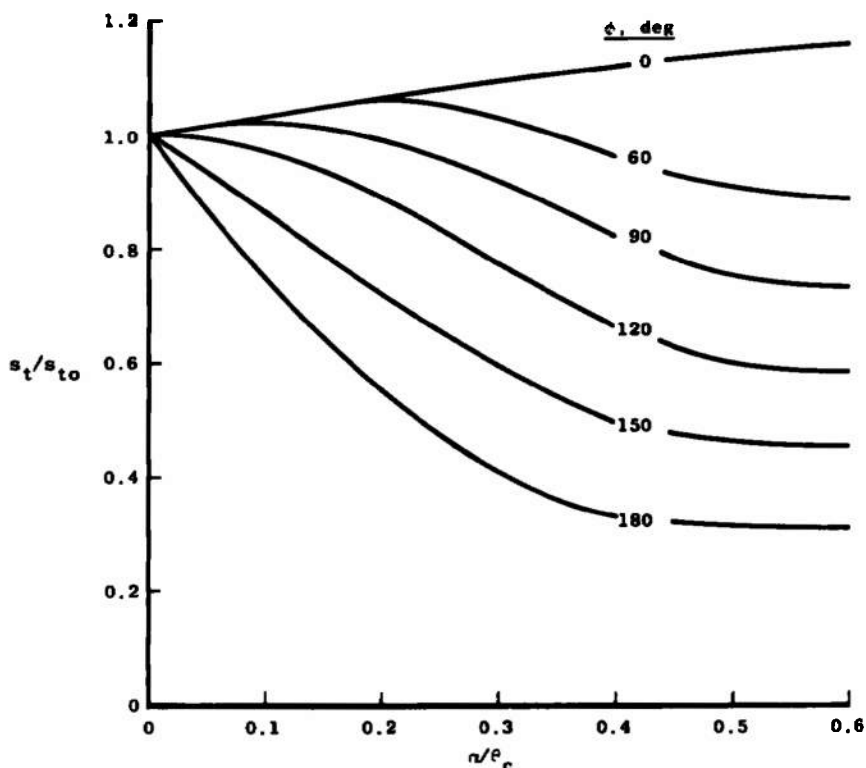
Figure 11. Combined data on angle-of-attack and meridian-angle influence.

In other words, Fig. 11 agrees with Ward for ϕ = 0 and 180, and the curves for intermediate values of ϕ are based on the replotted and re-faired data of DiCristina and Mateer.

In consideration of the foregoing, the procedure to be followed in accepting data and in adjusting the transition locations taken from shadowgrams of cones at variable α and ϕ follows:

(1) Use data for $\alpha/\theta_c \leq 0.3$ and all ϕ

(2) Present windward (low correction) data separately

(3) Make adjustments to obtain α = 0 results by using Fig. 11

(4) Disregard the effect of small angles of attack on local Mach and Reynolds numbers.

The angle α_p was determined by the aid of a plumb line photo-graphed in the field of view of the cones in flight. The total angle of attack α was obtained from the orthogonal shadowgrams which have precisely ruled grids in the field of view. Total angle was calculated

15

at each orthogonal shadowgram station, and a curve was fitted through those data so that the total angle could be read at the range stations where the photographs for transition study were made. It is known that the trajectory of the cones was essentially parallel to the plane of the film; i.e., the relative wind was nearly parallel to the film plane and aligned with the range axis.

The following sketch represents a cone in flight with its center of gravity, cg, moving in a path parallel to the plane of its photograph, with an angle of attack α_p measured in the photograph and a total angle of attack α between the body longitudinal axis of symmetry, x, and the relative wind, U_∞.
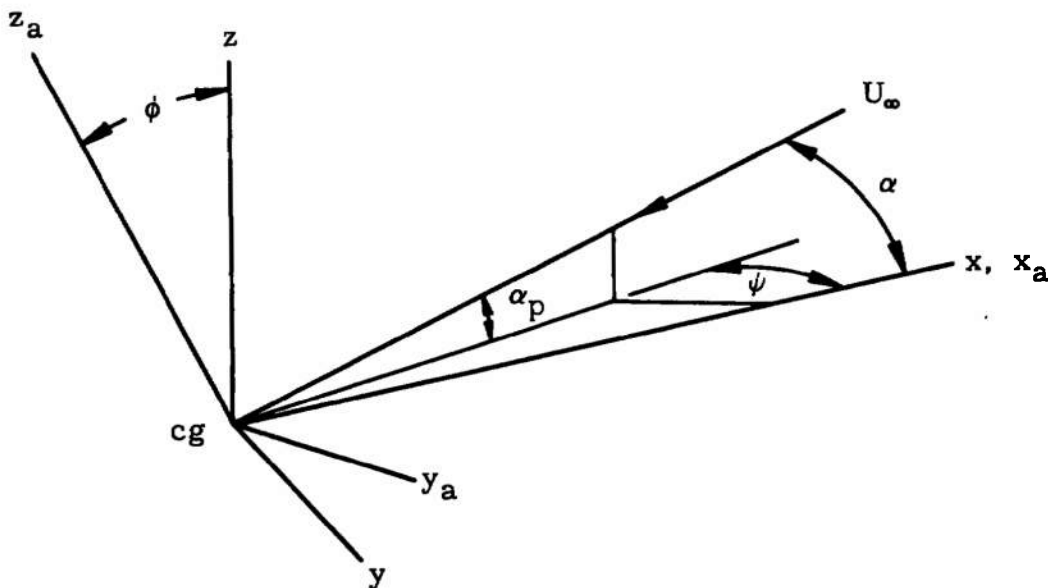
The aeroballistic axes (x_a, y_a, z_a) and the body axes (x, y, z) are arranged such that

x_a is coincident with the body axis x

y_a is orthogonal to x_a and z_a

z_a is orthogonal to x_a and y_a and lies in the plane of the total angle of attack α

x is coincident with the cone longitudinal axis of symmetry

y is orthogonal to x and z and is horizontal, i.e., normal to the photograph plane

z is orthogonal to x and y and is vertical in the plane of the photograph

The z axis lies in the plane of the cone meridians on the top and bottom of the silhouette in the photograph; i.e., the cone meridians on which transition is read. The z_a axis lies in the plane of the cone meridians corresponding to the windward and leeward stagnation lines. Therefore, ϕ is the circumferential angle between z and z_a or y and y_a. It is the angle needed so that one may take account of $\alpha_p \neq \alpha$ and adjust the windward and leeward transition readings accordingly.

The relationships are more simply illustrated in the following sketch:
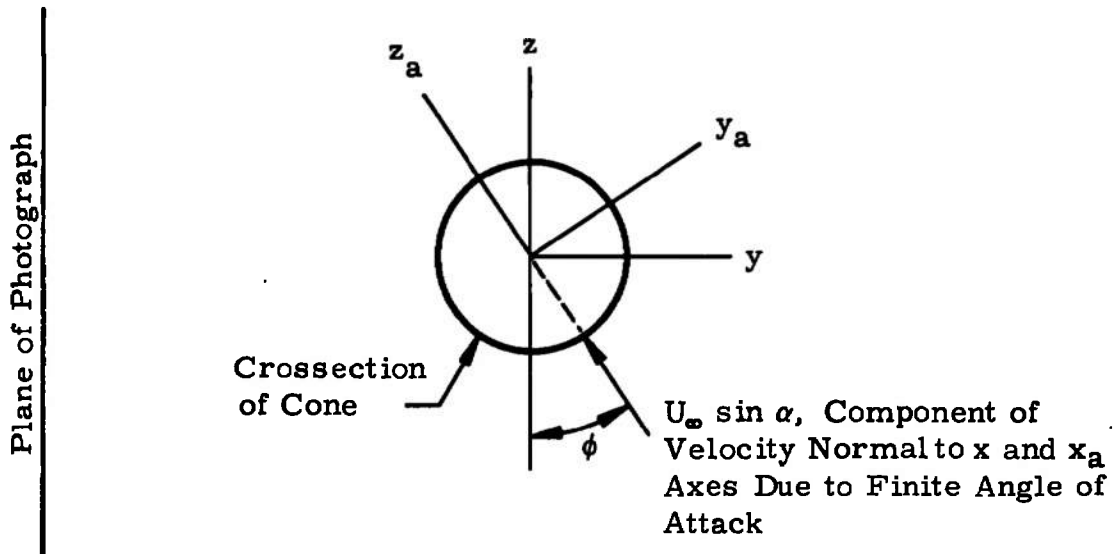
To develop the needed equation for ϕ, let the aeroballistic axes system be rotated about the y_a axis through the angle α so that the x_a axis coincides with the total velocity vector. Designate the resulting axes system with the subscript t. Then, a force along the x_t axis is expressible in terms of its force components along the x, y, z (body) axes according to the following equations:

$$Fx_t = Fx \cos\alpha + Fy \sin\alpha \sin\phi - Fz \sin\alpha \cos\phi \qquad (1)$$

or

$$Fx_t = Fx \cos\alpha_p \cos\psi + Fy \sin\psi + Fz \sin\alpha_p \cos\psi \qquad (2)$$

From whence it follows that

$$\cos \alpha = \cos \alpha_p \cos \psi \qquad (3)$$

$$\sin \alpha \sin \phi = \sin \psi \qquad (4)$$

$$\sin \alpha \cos \phi = \sin \alpha_p \cos \psi \qquad (5)$$

From Eqs. (3) to (5),

$$\cos \phi = \sin \alpha_p \cos \psi \,'\sin \alpha$$

or

$$\phi = \cos^{-1} (\sin \alpha_p \cos \psi \,'\sin \alpha) \qquad (6)$$

With all angles small, Eq. (6) reduces to

$$\phi \approx \cos^{-1} \alpha_p \,'\alpha \qquad (7)$$

Positive and negative signs have not been used because they are unnecessary. If both α and α_p are treated as positive angles, it is only necessary to remember that ϕ will represent the windward meridian and $180 - \phi$ will represent the leeward meridian in the shadowgrams. The angle ϕ is measured circumferentially starting from the windward stagnation line.

3.3 MEASUREMENT UNCERTAINTIES

The chief data in this research are comprised of transition locations determined by examination of shadowgrams of a number of individual cones in flight. The uncertainty in the visual process of locating transition and the inherent degree of nonrepeatability in such data combine to make the results virtually insensitive to the levels of uncertainty in most other supporting measurements. Cone velocity is accurate to within 0.04 percent; range pressure to within 1 percent; range temperature to within 0.5 K. Thus, the uncertainties in M_∞ and $(U/\nu)_\infty$ are of no consequence in these experiments. The same clearly is true of the physical dimensions of the cones. Only the angles of attack suffer from uncertainties in measurement which could affect the final, corrected results of this investigation. While α_p is accurate to within approximately 0.2 deg, the uncertainty in α may be as great as 0.5 deg in some cases. This should be remembered when

the influence of α on the transition Reynolds number is discussed. Although α_p and α will be given to the nearest 0.1 deg later, the uncertainty is several times that level. This introduces a random uncertainty in the transition Reynolds numbers which no doubt contributes to the scatter of the experimental results. However, as will be seen, it can not significantly bias the major findings.

3.4 THE DEFINITION OF TRANSITION IN SHADOWGRAMS

The object here is to describe the basis for selecting a "transition point" when looking at a shadowgram. First, it will be recalled that transition takes place over a finite length of the boundary layer, the transition region often being equally as long as the laminar flow region preceding it (cf. Potter and Whitfield, Ref. 9). Thus, it is not uncommon to refer to a beginning and an end of transition.

As usually defined, the beginning corresponds to the first (most upstream) departure from laminar flow while the end is at the downstream location where the characteristics of fully developed turbulent flow are first attained. It will be recognized that measurements within the boundary layer or on the surface adjacent to it are needed if such precise definitions are to be justified. When looking at a photograph of boundary layer transition, one can point to the most upstream evidence of disturbances to the laminar flow and a downstream station where the boundary layer first appears to become fully turbulent. Often there is doubt as to the precise stations where either of these stages of transition may be said to exist. The most upstream station may be confused with an early burst or moving spot or turbulence photographed at a location that would be found to be normally laminar if observed over a greater period of time. The end of the transition region may be difficult to identify in a photograph because of the gradual and subtle gradation leading to fully developed turbulence. By considering these problems, a single representative transition point was sought, based on the judgment that the downstream limit of laminar processes had been reached and that significant, continuing random processes had begun. This is not a definition that can be applied and defended in terms of fractions of inches. Fortunately, the nature of the results to be presented is such that rather wide bands of uncertainty on values of s_t can be tolerated.

Emphasis is placed on randomness in the boundary layer flow at transition. Laminar layers are known to exhibit both lateral and

longitudinal waviness or oscillations as the transition region is approached, and care must be taken to distinguish between the more orderly laminar motion and the random, disordered appearance of the transitional layer. In particular, occasional isolated turbulent spots followed downstream by laminar flow or regular, rope-like, vortical patterns sometimes seen in laminar flow are not defined as transition. Papers by Hama, et al. (Ref. 10) and Tani (Ref. 11) give detailed descriptions of the physical processes in transition. Klebanoff, et al. (Ref. 12), have contributed data on streamwise and spanwise flow patterns in laminar and transitional boundary layers. Benney and Lin (Ref. 13) succeeded in a mathematical derivation of secondary flow patterns such as those observed by Klebanoff, et al.

Figures 4 to 6 are typical shadowgrams obtained during this investigation. Negatives or enlarged prints were studied through a magnifying glass to establish transition location when processing the original data, but the reproductions in Figs. 4 to 6 convey an impression of the type of data obtained. Consistency in these readings is the most important virtue insofar as the investigation of unit Reynolds number effect is concerned. Nevertheless, it is believed that the transition locations also are relatively accurate, representative points for the transition process.

3.5 TEMPORAL AND SPATIAL VARIATION IN TRANSITION LOCATION

Data are available which show that the transition point as used herein, or any similar transition location, is subject to rather large, rapid fluctuations about some mean point with time. When one of the sensors of transition that effectively averages signals is used, or when a measurement such as total drag coefficient is taken, the temporal variations usually are concealed. However, when high-speed spark photography is used, one should expect to see considerable spread in the results even under fixed conditions. This is well illustrated in Fig. 12 which is based on measurements by Potter and Whitfield (Ref. 9). One will note the ±22 percent excursions in s_t about the mean station of transition. Similar data have been presented by Spangenberg and Rowland (Ref. 14) who found ±20 percent temporal variation about a mean transition location. The implication is that the present data based on single, short-duration spark photographs of cones in flight should be expected to display at least as much scatter in s_t values. Indeed, considering that each cone has some differences in motion compared to the others, it would be plausible for the data to spread even more than the ±22 percent seen in Fig. 12.
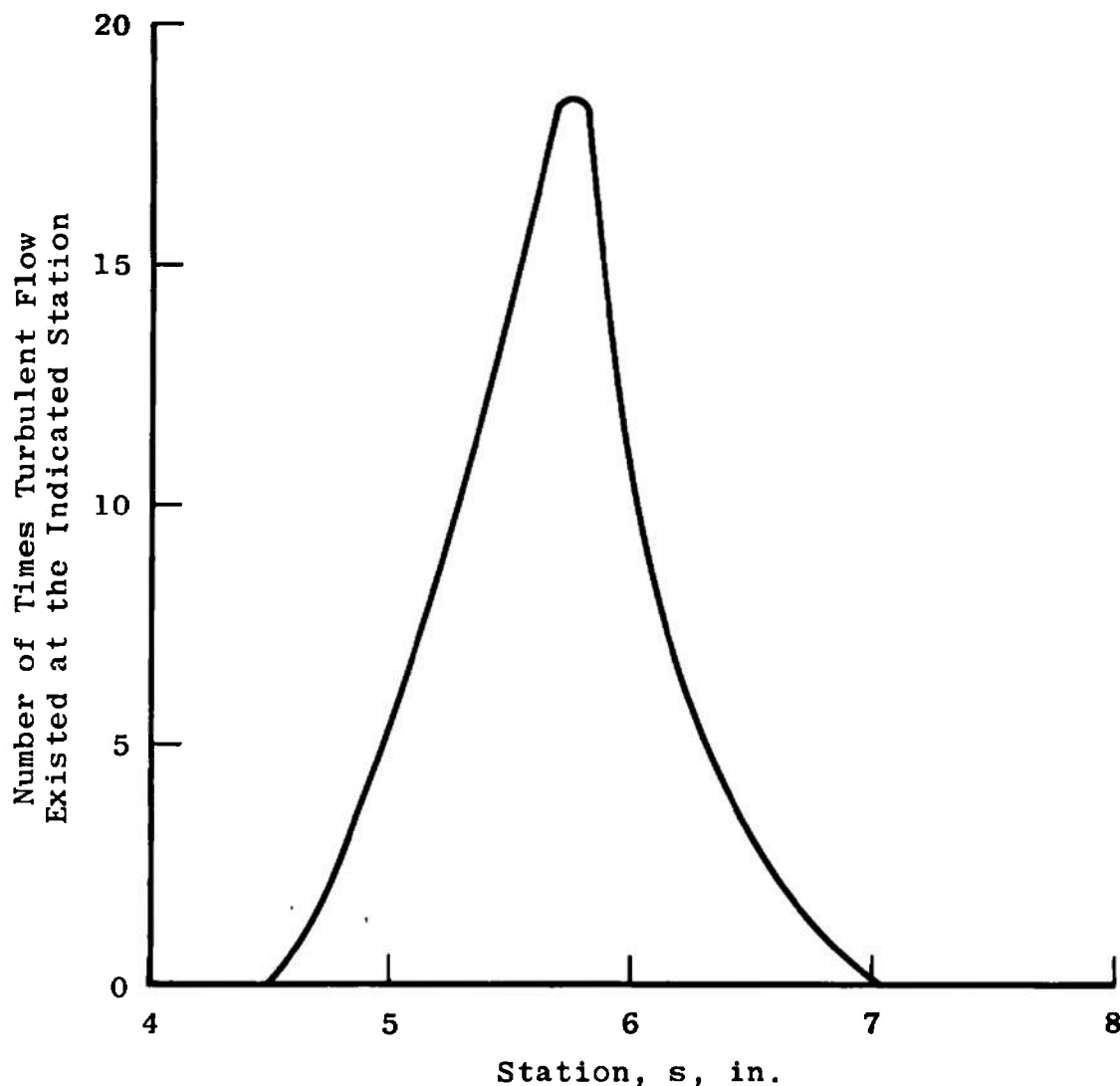
Figure 12. Experimental distribution of transition locations under
fixed flow conditions, based on Potter and Whitfield (Ref. 9).

In addition to the temporal phenomenon just discussed, it is equally
well known that a transition "line" typically traces an irregular pattern
laterally across a flat plate or circumferentially around a body of revo-
lution. That is illustrated in Fig. 13 which is taken from Ref. 2 and was
originally contributed by Dr. J. M. Kendall of the Jet Propulsion Labo-
ratory. What may at first appear to be badly scattered data will not
seem so unusual when the well recognized temporal and spatial restless-
ness of transition is taken into account. Each of the shadowgrams shows
a near-instantaneous picture of the unsteady transition region on two of
the meridians of a single cone.

21
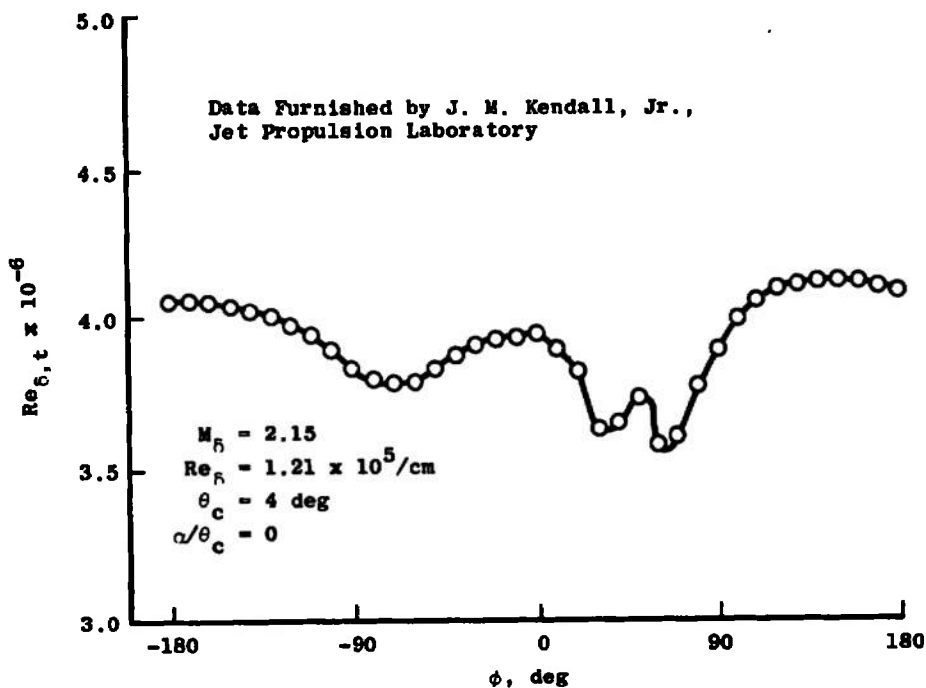
Figure 13. Circumferential variations in transition location on a cone at $\alpha = 0$.

3.6 BIAS INTRODUCED BY OBSERVING THE OUTER PART OF THE BOUNDARY LAYER

There is a variation in degree of turbulence along an axis normal to the surface on which the transitional boundary layer develops, cf. Potter and Whitfield (Ref. 9). The energy of turbulent fluctuations is distributed along this axis and has a maximum of some critical height, y_c. To see the influence of this on shadowgrams of the boundary layer, it is necessary to visualize a height in the boundary layer where the turbulence is first manifest and from whence it spreads downstream.

Again referring to Ref. 9, it has been shown that the critical height migrates outward, away from the solid boundary as Mach number increases. At the average local Mach numbers of the present report, the ratio of critical height to boundary layer thickness is

$$y_c'/\delta \approx 0.3$$

This suggests that turbulence generally exists at stations upstream of the region where "transition" is determined from examining flow photographs. However, the situation is not serious insofar as the error in transition locations is concerned. Reference 9 shows that the outer edge of the boundary layer deviated from the laminar growth rate within a few boundary layer thicknesses in length downstream of the station where turbulent fluctuations were found within the boundary layer, i.e.,

$$(s_t - s_i)/\delta_t < 0(10)$$

where s_t is identified as the beginning of transition indicated by flow photographs, s_i is the station where transition "starts" within the boundary layer at y_c, and δ_t is the thickness at s_t.

Following Ref. 15, it is calculated that

$$\delta = 0.005 \, s^{1/2} \text{ cm}$$

when

$$M_\delta = 0.90$$
$$(U'/\nu)_\delta = 0.35 \times 10^6 \text{ cm}^{-1}$$
$$T_w = T_\infty = 297 \text{ K}$$

and s is given in cm. Thus, it is conservative to state that

$$\delta_t < 0.1 \text{ cm}$$

and it follows that

$$s_t - s_i < 0(1 \text{ cm})$$

Values of s_t in this experiment were on the order of 10 cm; so it is considered that differences between s_t and s_i were not important in the identification of transition locations.

4.0 RESULTS AND CONCLUSIONS

Boundary layer transition locations determined by examination of shadowgrams were used in combination with the correction procedure

for α and ϕ and the computed local unit Reynolds numbers to yield the $Re_{\delta,t}$ values given in Table 1. Corresponding local Mach numbers also are given. Because the windward transition locations are subjected to much smaller α and ϕ corrections, those Reynolds numbers are listed separately from the averaged wind and lee data.

Table 1. Transonic Cone Boundary Layer Transition Data.[a]

Shot No.	M_∞	$\alpha,$ deg	$\alpha_p,$ deg	$(U/\nu)_\delta \times 10^{-6}$	M_δ	C_{D_o}	$Re_{\delta,t} \times 10^{-6}$	
2832	1.04	2.5	2.5	0.43 per cm	0.88	0.56	4.6[b]	5.7[c]
2833	1.05	2.8	0.3	0.35 per cm	0.90	0.53	5.1[b]	5.3[c]
2834	1.05	2.7	0.9	0.35 per cm	0.90	0.54	4.7[b]	4.7[c]
2846	1.11	2.5	0.0	0.48 per cm	0.94	0.55	4.3[b]	4.8[c]
2845	1.11	2.0	1.7	0.27 per cm	0.94	0.53	3.8[b]	4.3[c]
2839	1.25	2.2	0.7	0.37 per cm	1.15	0.46	4.1[b]	4.3[c]
2743	1.30	1.4	1.4	0.28 per cm	1.17	0.46	>3.6	>3.6
2835	1.44	1.7	0.2	0.55 per cm	1.28	0.42	5.3[b]	5.3[c]

[a]For a nominally sharp, smooth cone with semiapex angle = 10 deg and $T_\infty = T_w$ = 300 K in an aeroballistic range.
[b]Only windward-side data, corrected for α and ϕ effects.
[c]Average of wind and lee data after correction for α and ϕ effects.

Figure 14 shows the present transonic data plotted for comparison with the aeroballistic range data of Refs. 1 and 2. Also shown are two different forms of least-squares, data-fitting curves which were derived to fit the data of Refs. 1 and 2. The two curves, which fit the older data equally well, emphasize the hazard of extrapolating the data, particularly toward lower unit Reynolds numbers where the two curves rapidly diverge. Unfortunately, the curtailment of the experimental program prevented getting transition data at lower unit Reynolds numbers. Therefore, it is not possible to say if $Re_{\delta,t}$ under the aeroballistic range conditions would continue to decline or approach a lower limit just above 3×10^6 at still lower $(U/\nu)_\delta$. This question, as well as the apparent tendency for

$$Re_{\delta,t} \approx \text{const. for given } (U/\nu)_\delta$$

at

$$0.9 \leq M_\delta \leq 4.3$$

with

$$T_w = T_\infty \text{ at all } M_\delta$$

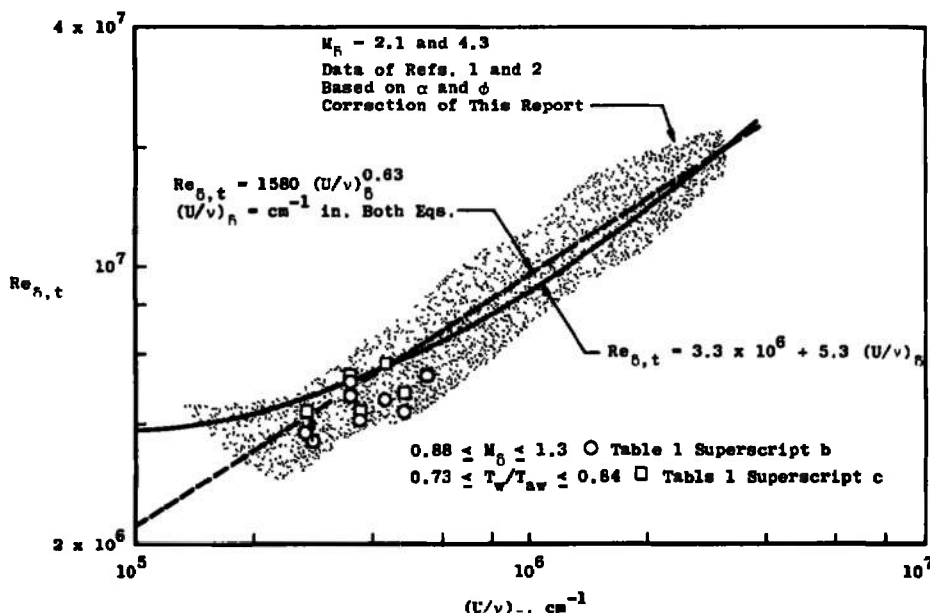deserves additional study.

Figure 14. Transonic transition data compared with other data for 10-deg semiangle cones in AEDC Range K.

This report would seem incomplete without any comparison of these data with wind tunnel results on cones for comparable Mach and unit Reynolds numbers. Such a comparison is included, partly to satisfy the curiosity of experimenters, but it must be hedged with caveats. That is because of differences in factors which may affect the Reynolds number of transition and which cannot be evaluated with any confidence at this time. For example, it is apparent that the disturbance intensity and spectrum imposed on boundary layers in wind tunnels generally differs between wind tunnels and certainly is not the same as exists in aeroballistic ranges. This may be of major importance. In addition, it is usual for model wall temperature, T_w, to be close to adiabatic recovery temperature, T_{aw}, in most transonic wind tunnels. In contrast, the aeroballistic range condition of $M_\infty = 1.05$ and $T_w = T_\infty$ gives

$$T_w/T_{aw} = 0.84$$

25

At $M_\infty = 1.44$ and $T_w = T_\infty$,

$$T_w/T_{aw} = 0.73$$

The influence of different wind tunnel and range disturbance environments cannot be evaluated because, first, those environments are not adequately defined and, second, even if the characteristics were known more fully, the effect on transition would not be predictable at the present state of the art. In a very incomplete way, the wind tunnel and range disturbances may be compared as shown in Fig. 15 where one is warned not to ignore differences in parameters other than ΔC_p.
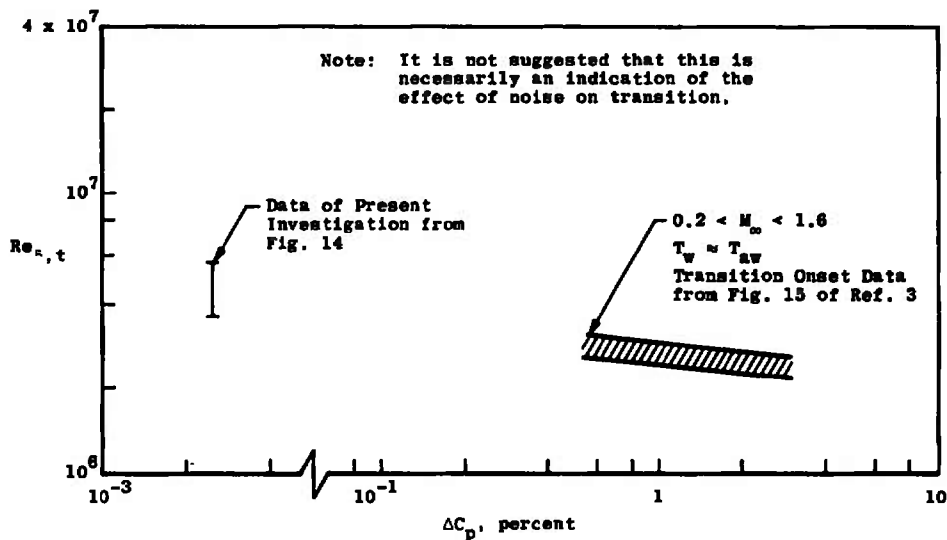
Figure 15. Comparison of noise in range and transonic wind tunnel.

The wind tunnel data in Fig. 15 are from Ref. 3 and are generally indicative of data from other large transonic wind tunnels reported therein. The parameter,

$$\Delta C_p = \left(\sqrt{\overline{p^2}}/q_\infty\right) \times 100 \quad , \quad \text{percent}$$

represents the ratio of time-averaged, frequency-integrated, rms, fluctuating pressure to the free-stream dynamic pressure,

$$q_\infty = (\gamma/2)p_\infty M_\infty^2$$

Measurements of $\sqrt{\tilde{p}^2}$ were made in the present aeroballistic experiments, and it was found that $\Delta C_p \lesssim 0.0025$ percent. Inasmuch as ΔC_p in the free-flight case was found to be far below the transonic wind tunnel values which vary around 1 percent, some would be led to conclude that, of course, $Re_{\delta,t}$ should be greater in the aeroballistic range than in a wind tunnel. Such conclusions were freely expressed after publication of Ref. 1, but they fail to account for the many possible sources of disturbances which may affect boundary layer transition.

For equal conditions of Mach number, unit Reynolds number, and wall temperature ratio, similar full-scale, free-flight, conical vehicles would be expected to experience transition Reynolds numbers essentially equal to those reported here. However, differences in nose bluntness, surface finish, vibration, etc., should not be overlooked in using these data for prediction of transonic transition on full-scale, free-flight vehicles.

REFERENCES

1. Potter, J. Leith. "Observations on the Influence of Ambient Pressure on Boundary-Layer Transition." AEDC-TR-68-36 (AD666911), March 1968.

2. Potter, J. Leith. "Studies of Boundary-Layer Transition on Aeroballistic Range Models." AEDC-TR-73-194 (AD778841), May 1974.

3. Dougherty, N. S., Jr. and Steinle, Frank W., Jr. "Transition Reynolds Number Comparisons in Several Major Transonic Tunnels." AIAA Paper No. 74-627, AIAA 8th Aerodynamic Testing Conference, Bethesda, Maryland, July 8-10, 1974.

4. Ames Research Staff. "Equations, Tables, and Charts for Compressible Flow." NACA Report 1135, 1953.

5. Kendall, J. M., Jr. "Wind Tunnel Experiments on Fluctuation Sources and Amplification Rates in Supersonic and Hypersonic Boundary Layers." AIAA Paper 74-133, February 1, 1974.

6. Ward, L. K. "Influence of Boundary-Layer Transition on Dynamic Stability at Hypersonic Speeds." Transactions of the Second Technical Workshop on Dynamic Stability Testing, Arnold Engineering Development Center, Vol II (AD472298), April 1965.

7. Mateer, G. C. "Effects of Wall Cooling and Angle of Attack on Boundary Layer Transition on Sharp Cones at $M_\infty = 7.4$." NASA TN D-6908, August 1972.

8. DiCristina, V. "Three-Dimensional Laminar Boundary-Layer Transition on a Sharp 8-deg Cone at Mach 10." AIAA Journal, Vol. 8, No. 5, May 1970, pp. 852-856.

9. Potter, J. L. and Whitfield, J. D. "Effects of Slight Nose Bluntness and Roughness on Boundary-Layer Transition in Supersonic Flows." Journal of Fluid Mechanics, Vol. 12, Part 4, 1962, pp. 501-535.

10. Hama, F. R., Long, J. D., and Hegarty, J. C. "On Transition from Laminar to Turbulent Flow." Journal of Applied Physics, Vol. No. 28, 1957, p. 388.

11. Tani, I. "Boundary Layer Transition." Annual Review of Fluid Mechanics, (W. R. Sears, ed.), Vol. No. 1, 1969, p. 169, Annual Reviews, Palo Alto, California.

12. Klebanoff, P. S., Tidstrom, J. D., and Sargent, L. M. "The Three-Dimensional Nature of Boundary Layer Instability." Journal of Fluid Mechanics, Vol. No. 12, 1962, p. 1.

13. Benney, D. J. and Lin, C. C. "On the Secondary Motion Induced by Oscillations in a Shear Flow." Physics of Fluids, Vol. No. 3, 1960, p. 656.

14. Spangenburg, W. G., and Rowland, W. R. "Optical Study of Boundary Layer Processes in a Supersonic Air Stream." Physics of Fluids, Vol. No. 3, 1960, p. 667.

15. Cohen, C. B., and Reshotko, E. "The Compressible Laminar Boundary Layer with Heat Transfer and Arbitrary Pressure Gradient." NACA Report 1294, 1956.

NOMENCLATURE

C_{D_o}	Total drag coefficient adjusted to zero angle of attack
ΔC_p	$\sqrt{\tilde{p}^2}/q_\infty$
M	Mach number
p	Pressure
$\tilde{p}$	Fluctuating sound pressure amplitude
q_∞	Free-stream dynamic pressure
Re	Reynolds number
s	Distance measured along surface from stagnation point
T	Temperature
U	Velocity
α	Total angle of attack
α_p	Angle of attack in plane of photograph
γ	Ratio of specific heats
δ	Boundary layer thickness
θ_c	Cone semi-apex angle
ν	Kinematic viscosity
ρ	Mass density
ϕ	Orientation of a cone meridian relative to the windward stagnation line where $\phi = 0$

SUBSCRIPTS

aw	Adiabatic wall
o	Total, e.g., total temperature; also designates $\alpha = 0$
t	Transition
w	Cone wall
α	Denotes $\alpha \neq 0$
δ	Local flow parameter at outer edge of boundary layer
∞	Free stream